Production of in vivo-biotinylated rotavirus particles

De Lorenzo, G ; Eichwald, C ; Schraner, E M ; Nicolin, V ; Bortul, R ; Mano, M ; Burrone, O R ; Arnoldi, F

Abstract: Although inserting exogenous viral genome segments into rotavirus particles remains a hard challenge, this study describes the in vivo incorporation of a recombinant viral capsid protein (VP6) into newly assembled rotavirus particles. In vivo biotinylation technology was exploited to biotinylate a recombinant VP6 protein fused to a 15 aa biotin-acceptor peptide (BAP) by the bacterial biotin ligase BirA contextually co-expressed in mammalian cells. To avoid toxicity of VP6 overexpression, a stable HEK293 cell line was constructed with tetracycline-inducible expression of VP6-BAP and constitutive expression of BirA. Following tetracycline induction and rotavirus infection, VP6-BAP was biotinylated, recruited into viroplasms and incorporated into newly assembled virions. The biotin molecules in the capsid allowed the use of streptavidin-coated magnetic beads as a purification technique instead of CsCl gradient ultracentrifugation. Following transfection, double-layered particles attached to beads were able to induce viroplasm formation and to generate infective viral progeny.

DOI: https://doi.org/10.1099/vir.0.040089-0

Journal of General Virology (2012), **93**, 1474–1482 **DOI** 10.1099/vir.0.040089-0

Production of *in vivo*-biotinylated rotavirus particles

G. De Lorenzo,[1] C. Eichwald,[2] E. M. Schraner,[2,3] V. Nicolin,[4] R. Bortul,[4] M. Mano,[1] O. R. Burrone[1] and F. Arnoldi[1,4]

Correspondence
O. R. Burrone
Oscar.Burrone@icgeb.org
F. Arnoldi
farnoldi@units.it

[1]International Centre for Genetic Engineering and Biotechnology (ICGEB), Padriciano 99, 34149 Trieste, Italy

[2]Institute of Virology, University of Zürich, Winterthurerstrasse 260, CH-8057 Zürich, Switzerland

[3]Institute of Veterinary Anatomy, University of Zürich, Winterthurerstrasse 260, CH-8057 Zürich, Switzerland

[4]Dipartimento Universitario Clinico di Scienze Mediche, Chirurgiche e della Salute, Strada di Fiume 447, 34149 Trieste, Italy

Received 25 November 2011
Accepted 16 March 2012

Although inserting exogenous viral genome segments into rotavirus particles remains a hard challenge, this study describes the *in vivo* incorporation of a recombinant viral capsid protein (VP6) into newly assembled rotavirus particles. *In vivo* biotinylation technology was exploited to biotinylate a recombinant VP6 protein fused to a 15 aa biotin-acceptor peptide (BAP) by the bacterial biotin ligase BirA contextually co-expressed in mammalian cells. To avoid toxicity of VP6 overexpression, a stable HEK293 cell line was constructed with tetracycline-inducible expression of VP6–BAP and constitutive expression of BirA. Following tetracycline induction and rotavirus infection, VP6–BAP was biotinylated, recruited into viroplasms and incorporated into newly assembled virions. The biotin molecules in the capsid allowed the use of streptavidin-coated magnetic beads as a purification technique instead of CsCl gradient ultracentrifugation. Following transfection, double-layered particles attached to beads were able to induce viroplasm formation and to generate infective viral progeny.

INTRODUCTION

Rotavirus is the most common aetiological agent of gastroenteritis in infants and young children worldwide (Dennehy, 2008). The virion is a non-enveloped, triple-layered particle (TLP) containing a genome of 11 segments of dsRNA encoding six structural proteins (VP1–VP4, VP6 and VP7) and, depending on the virus strain, five or six non-structural proteins (NSP1–NSP6) (Estes & Kapikian, 2007). The RNA genome together with the enzymes required for transcription and genome replication (VP1 and VP3) are packaged inside the virion, surrounded by three concentric protein layers (Chen *et al.*, 1999; Liu *et al.*, 1992; Pizarro *et al.*, 1991; Valenzuela *et al.*, 1991). The outer layer consists of VP7 with spikes of VP4 trimers, whilst the intermediate layer is formed by VP6 and the inner one by VP2 (Lawton *et al.*, 1997a; Prasad *et al.*, 1996).

Following cell entry, the outer-layer proteins VP4 and VP7 are removed, resulting in a double-layered particle (DLP) that contains the second layer formed by 260 VP6 trimers associated in a T13 levo-icosahedral lattice (Lawton *et al.*, 1997b). DLPs are transcriptionally active and yet require the VP6 layer in addition to the enzymes directly involved in RNA synthesis. The exact role of VP6 in this process is not known (Bican *et al.*, 1982; Charpilienne *et al.*, 2002; Feng *et al.*, 2002; Lawton *et al.*, 1999; Libersou *et al.*, 2008; Thouvenin *et al.*, 2001). Furthermore, VP6 may have a role during budding of DLPs from viroplasms, the cytoplasmic virus factories in which they form, into the endoplasmic reticulum where they acquire the third layer (Delmas *et al.*, 2004; Meyer *et al.*, 1989; Taylor *et al.*, 1992, 1993). The crystal structure of VP6 has been determined (Mathieu *et al.*, 2001), and its interactions with the outer and inner layers have been described by biochemical (Charpilienne *et al.*, 2002) and structural (Chen *et al.*, 2009; Settembre *et al.*, 2011) studies. The VP6 monomer is folded into two different domains, an upper β-barrel domain and an α-helical domain, which participate in trimer stabilization and interactions with the outer and inner layers of the virion, respectively (Mathieu *et al.*, 2001). The VP6 trimer has a tower-like shape whose base shows a triangular cross-section, whilst the head has a hexagonal cross-section. Each of the three VP6 molecules exposes three loops (A′A″, BC and HI) for interaction with the VP7 outer layer (Mathieu *et al.*, 2001). In the present work, we describe insertion into the loop HI of an exogenous 15 aa biotin-acceptor peptide (BAP) that allowed *in vivo* biotinylation of the modified protein. The BAP peptide was specifically biotinylated *in vivo* when contextually co-expressed in mammalian cells with the *Escherichia coli*-derived biotin ligase, BirA (Beckett *et al.*, 1999). BirA covalently attaches a single biotin molecule to a defined lysine residue within BAP. We have

shown previously that both cytosolic and secretory BAP-tagged proteins can be efficiently biotinylated when BirA is targeted either to the cytosol or to the secretory pathway, respectively (Petris *et al.*, 2011; Predonzani *et al.*, 2008). Here, we describe the incorporation of *in vivo*-biotinylated VP6–BAP into newly assembled viral particles resulting in functional DLPs and TLPs decorated with biotin molecules.

RESULTS AND DISCUSSION

In vivo-biotinylated VP6 trimerizes and localizes in viroplasms

We constructed a recombinant VP6 protein by modifying a site within loop HI, which should not be involved in proper folding (Mathieu *et al.*, 2001). The BAP peptide, flanked by 2 aa upstream (SG) and 3 aa downstream (GAS), was inserted between residues P309 and P313 of VP6 from the simian rotavirus SA11 strain, replacing residues N310, A311 and Q312, which are not involved in intra-trimer contacts (Mathieu *et al.*, 2001) (Fig. 1a). The position in which BAP was inserted within the VP6 structure should allow the addition of biotin molecules on the surface of DLPs.

In order to obtain recombinant viral particles containing the BAP-tagged VP6 protein (VP6–BAP), rotavirus-infected cells expressing this recombinant protein were needed. Numerous attempts to obtain a stable cell line constitutively expressing VP6–BAP failed, probably because of the toxicity of the cytosolic tubules formed by VP6 when overexpressed alone (Contin *et al.*, 2010; Lepault *et al.*, 2001). To address this problem, the VP6–BAP gene was cloned under the control of a tetracycline-inducible promoter (TetOn). We used the Flp-In T-REx system (Life Technologies) designed for rapid generation of stable HEK293 cell lines through site-specific genome integration mediated by the enzyme flippase (Flp) (O'Gorman *et al.*, 1991). A genetic construct was derived containing, in addition to the tetracycline-inducible VP6–BAP gene, a constitutive transcriptional unit for the cytosol-localized enzyme BirA (cytBirA) (Fig. 1b). We first checked, by transient transfection into HEK293 cells, whether VP6–BAP was biotinylated by the BirA enzyme and was still capable of forming trimers. As shown in the Western blot retardation assay in Fig. 1(c, left panel), VP6–BAP was very efficiently biotinylated by BirA. In this assay, proteins were resolved by SDS-PAGE in the presence of streptavidin. The complex formed by biotinylated proteins and streptavidin is resistant to denaturing conditions and therefore only biotinylated molecules showed a retarded migration. All VP6–BAP molecules were found to be retarded, thus indicating a biotinylation efficiency close to 100 %. It was also observed that VP6–BAP was able to form trimers (Fig. 1c, right panel), indicating that an important feature required for proper assembly of the second layer in virus particles was preserved.

A stable transfectant (HEK293/VP6–BAP) was then established, containing two characteristics: (i) constitutive expression of BirA, and (ii) tetracycline-inducible expression of VP6–BAP. The level of VP6–BAP expression, however, was very low. In fact, as shown in Fig. 1(d), although VP6–BAP could be detected with HRP-conjugated streptavidin, its expression level was below the threshold for detection with the anti-VP6 serum, which nevertheless reacted with wild-type VP6 in infected cells. Therefore, in these cells, virus replication would take place with a highly unbalanced contribution of VP6–BAP in relation to the wild-type protein.

In spite of this, when these cells were induced with tetracycline and infected the day after with rotavirus SA11 strain, we observed that VP6–BAP was able to localize in viroplasms. As shown in Fig. 1(e), only after tetracycline treatment was biotinylated VP6–BAP detected at the periphery of viroplasms, which were stained with antibodies reacting with the viroplasm-resident protein NSP5. These results indicated that biotinylated VP6–BAP has the capacity to be recruited into viroplasms, as occurs with the wild-type protein.

In vivo-biotinylated VP6 is incorporated into newly synthesized viral particles

In order to investigate whether VP6–BAP could also be incorporated into viral particles, tetracycline-induced cells were infected for 48 h (m.o.i. of 3), and newly formed viral particles were then purified by CsCl gradient ultracentrifugation. Fractions of the gradient corresponding to TLPs, DLPs and empty particles not containing the viral genome (EPs) were analysed by Western blotting for the presence of biotinylated VP6–BAP (Fig. 2a). VP6–BAP was found in all three types of viral particles only when infection occurred in the presence of tetracycline. Interestingly, both TLPs and DLPs, distinguished because of the presence of VP7 in TLPs, contained biotinylated VP6–BAP, indicating that the presence of biotinylated VP6–BAP molecules in addition to wild-type VP6 did not interfere with formation of the outer shell. This finding was particularly important because, according to reconstruction of the VP6–VP7 heterohexamer based on high-resolution electron cryo-microscopy analysis of VP7-recoated DLPs, the VP6 loop containing the biotinylated BAP should be in close contact with VP7 (Chen *et al.*, 2009). Therefore, the small size of the tag used may have been crucial in order not to compromise the interaction with VP7. When observed by electron microscopy (uranyl acetate staining), the morphology of viral particles isolated from tetracycline-induced cells appeared almost identical to those isolated from non-induced cells (Fig. 2b). Furthermore, those fractions of the gradient found to contain a mixture of TLPs and DLPs were analysed by non-denaturing agarose gel electrophoresis in MOPS buffer (Fig. 2c). Under these conditions, TLPs and DLPs migrated as intact particles at different positions and could be visualized by ethidium bromide staining because

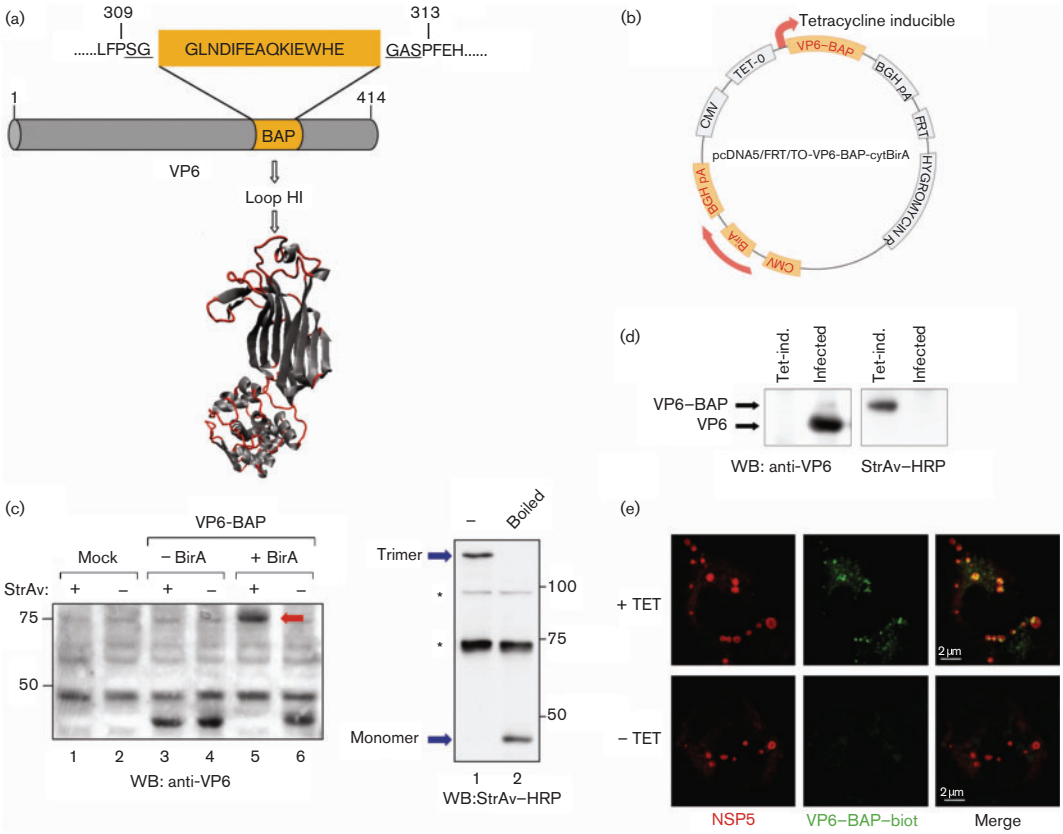

Fig. 1. *In vivo* biotinylation of VP6–BAP. (a) Top: schematic representation of the linear amino acid sequence of VP6–BAP; aa 310–312 (NAQ) were replaced with the 15 aa BAP peptide, indicated in the orange box, and the five amino acids used as linkers (underlined). Bottom: ribbon diagram of the VP6 monomer indicating the loop HI where BAP was located. (b) Schematic of the plasmid used to stably transfect Flp-In HEK293 cells resulting in constitutive expression of BirA and tetracycline-inducible expression of VP6–BAP. (c) Left panel: Western blot retardation assay of cellular extracts of HEK293 cells transiently transfected with the plasmid shown in (b) (lanes 5 and 6) or with the same plasmid without the BirA transcriptional unit cassette (lanes 3 and 4), pre-incubated with or without streptavidin (StrAv) before PAGE and analysed with anti-VP6 serum; the arrow indicates the shifted VP6–BAP molecules. Right panel: Western blot of biotinylated VP6–BAP revealed with streptavidin–HRP, not boiled (lane 1) or boiled (lane 2) before PAGE to visualize VP6–BAP trimers and monomers, respectively; asterisks indicate endogenous biotinylated proteins. (d) Western blot with anti-VP6 serum and streptavidin–HRP of extracts from tetracycline-induced cells (Tet-ind.) or virus-infected cells (Infected). (e) Confocal microscopy of Flp-In HEK293 cells stably transfected with the plasmid shown in (b), induced or not with tetracycline for 24 h, infected with rotavirus SA11 strain, and analysed for the presence of viroplasms (anti-NSP5, red) and biotinylated VP6–BAP (streptavidin–Alexa Fluor 488, green) at 5 h post-infection (p.i.).

of their RNA genome content (Fig. 2c, upper panel). The viral particles were then denatured by soaking the gel in a 1 % SDS solution and transferred from the agarose gel to a PVDF membrane in order to reveal the presence of biotinylated VP6–BAP by reacting with HRP-conjugated streptavidin. As expected, VP6–BAP was found in viral particles derived from tetracycline-induced infected cells and was absent in those coming from non-induced infected cells (Fig. 2c, middle panel). Whilst both TLPs and DLPs were shown to contain biotinylated VP6–BAP, biotin was displayed only on the surface of DLPs, as the addition of streptavidin-coated beads depleted them from the DLP/TLP mixture (Fig. 2c, middle panel, lane 4). Taken together, these data demonstrated that biotinylated VP6–BAP was incorporated into newly assembled viral particles.

Purification of biotinylated DLPs with streptavidin-coated magnetic beads

We took advantage of the high affinity between biotin and streptavidin to purify DLPs containing biotinylated VP6–BAP. We used magnetic beads coated with streptavidin on crude viral preparations, previously dialysed and treated with EDTA to convert TLPs into DLPs, thus increasing the yield of DLPs bearing VP6–BAP. The purified material was analysed by Western blotting with antibodies against VP1,

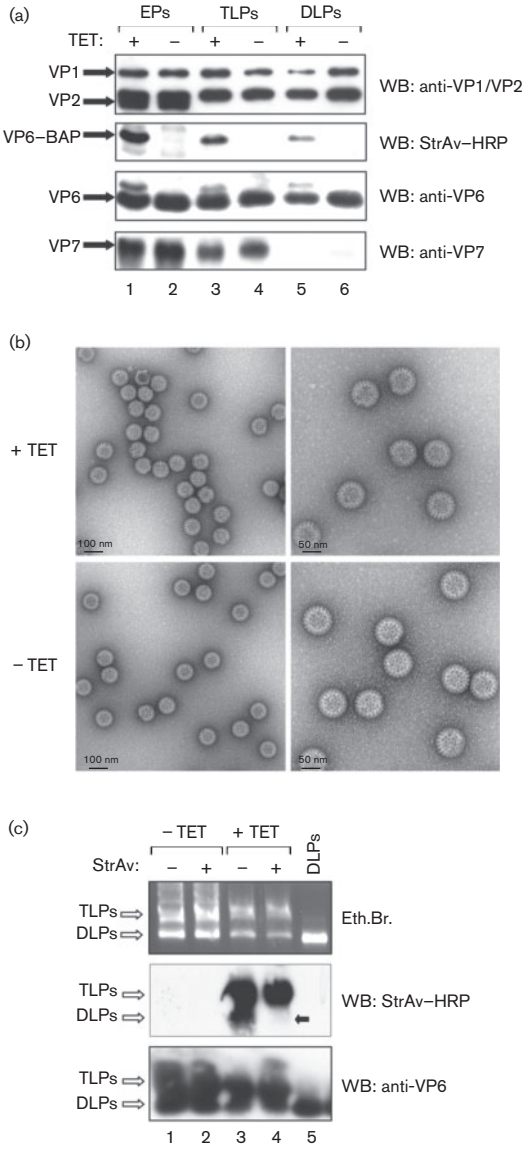

Fig. 2. Incorporation of biotinylated VP6–BAP into newly assembled viral particles. (a) Purification of rotavirus particles (TLPs, DLPs and EPs) by CsCl gradient ultracentrifugation and analysis by Western blotting with the indicated antibodies and with streptavidin–HRP. Viral particles were obtained from the SA11-infected HEK293/VP6–BAP stable cell line, induced or not with tetracycline (TET). (b) Electron microscopy (uranyl acetate staining) of DLPs purified as described in (a) from tetracycline-induced (upper panel) or non-induced (lower panel) HEK293/VP6–BAP cells. Bars, 100 nm (left panels); 50 nm (right panels). (c) DLPs and TLPs resolved by non-denaturing agarose gel electrophoresis and visualized by viral genome staining with ethidium bromide (Eth.Br.) (upper panel) and, after blotting onto a PVDF membrane, with anti-VP6 serum and, after stripping, with streptavidin–HRP (lower and middle panels, respectively). Where indicated, streptavidin-coated beads were added to sequester particles displaying biotin on their surface. The black arrow indicates the absence of biotinylated DLPs in lane 4.

VP2, VP7 and VP6 and with HRP-conjugated streptavidin. As shown in Fig. 3(a), successful purification of DLPs produced in tetracycline-induced cells was achieved in a single affinity-purification step, as revealed by Western blotting for the structural proteins VP1, VP2 and VP6. As expected, no biotinylated VP6–BAP was found in the unbound material (Fig. 3a, lane 5), represented by DLPs not containing VP6–BAP plus all viral proteins in excess, including soluble VP7 derived from the EDTA treatment. The absence in the purified material of NSP5, a viral protein abundantly expressed during infection but not incorporated in mature virions, further confirmed the specificity of the purification method. These results indicated that purification with streptavidin-coated magnetic beads can be used directly to obtain DLPs from total crude preparations, without the need for laborious CsCl ultracentrifugation. Comparing the yield of VP1 recovered in the purified fraction in relation to the unbound fraction, we estimated that around 35 % of all DLPs produced contained VP6–BAP and were therefore purified by the beads (Fig. 3a, compare the band intensity of VP1 in lanes 3 and 5). This quantification, however, underestimates the percentage of biotinylated viral particles because it also takes into account soluble viral proteins present in the unbound fraction. A better estimate was obtained by comparing VP1 levels between DLPs that were previously purified by CsCl gradient ultracentrifugation from tetracycline-induced and virus-infected cells under the same conditions as before, and then precipitated with streptavidin-coated magnetic beads. As shown in Fig. 3(b), around 90 % of DLPs contained VP6–BAP. Instead, CsCl-purified TLPs showed a lower level of particles containing VP6–BAP. As shown in Fig. 3(c), TLPs containing VP6–BAP represented around 40 % of the total. In order to determine the relative abundance of recombinant VP6–BAP (in relation to VP6) incorporated in DLPs, we used particles purified with streptavidin-coated magnetic beads to isolate only DLPs containing biotinylated VP6–BAP. The precipitated material was denatured by boiling in the presence of SDS, and both biotinylated VP6–BAP and VP6 were detected in Western blots (Fig. 3d). We took advantage of the different migration of VP6–BAP and VP6 in PAGE to reveal the two proteins with the same anti-VP6 antibody. Comparing the intensity of VP6–BAP in Fig. 1(d, lane 1) with that of VP6 in the serial dilutions, we estimated that VP6–BAP represented around 1–3 % of the total VP6. Thus, considering that VP6 is present in 780 copies per particle, DLPs were decorated, on average, with around eight to 25 biotin molecules per particle. This level of incorporated recombinant protein was the consequence of the very low expression of VP6–BAP in tetracycline-induced cells, as mentioned above (Fig. 1d).

In addition, as VP6–BAP was also observed in TLPs, the low incorporation rate may determine a condition of permissiveness for the assembly of the VP7–VP4 outer shell, in spite of the position in which BAP was inserted.

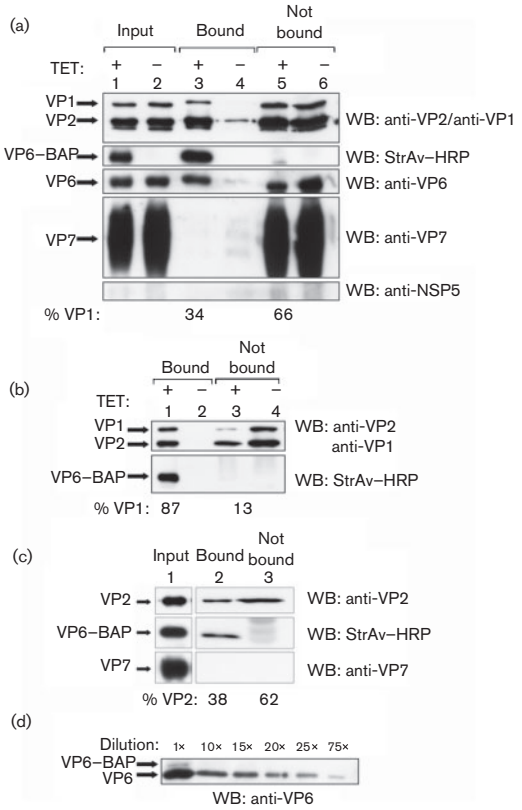

Fig. 3. Purification of TLPs and DLPs containing VP6–BAP. (a) Western blot with streptavidin–HRP and the indicated antibodies of DLPs purified with streptavidin-coated magnetic beads from tetracycline-induced or non-induced HEK293/VP6–BAP SA11-infected cells. The input (lanes 1 and 2) represents one-sixth of both the purified (lanes 3 and 4) and the unbound (lanes 5 and 6) material. Numbers below the blot show the percentage of purified VP1 (lane 3) and unbound VP1 (lane 5) compared with total VP1 (lane 3 + lane 5). (b) Western blot with the indicated antibodies and streptavidin–HRP of CsCl-purified DLPs precipitated with streptavidin-coated magnetic beads. Numbers below the blot show the percentage of purified VP1 (lane 1) and unbound VP1 (lane 3) compared with total VP1 (lane 1 + lane 3). (c) Western blot with the indicated antibodies and streptavidin–HRP of CsCl-purified TLPs. TLPs were converted into DLPs by EDTA treatment, pelleted by ultracentrifugation, resuspended and then isolated with streptavidin-coated magnetic beads. Numbers below the blot show the percentage of purified VP2 (lane 2) and unbound VP2 (lane 3) compared with total VP2 (lane 2 + lane 3). (d) Western blot with the anti-VP6 serum of serially diluted DLPs containing VP6–BAP purified with streptavidin-coated magnetic beads. In all cases, the band intensities were quantified using ImageJ software.

Viral particles containing biotinylated VP6–BAP are functional

In order to determine whether the affinity-purified DLPs were functionally active, we transfected them into cells and analysed their ability to form viroplasms and to produce infective particles. As shown in Fig. 4(a), transfection of DLPs not detached from beads led to the formation of viroplasms, as revealed at 5 h post-transfection with anti-NSP5 antibodies. The magnetic beads could be visualized in transfected cells, as indicated with arrows in Fig. 4. The formation of viroplasms was only observed when magnetic beads were incubated with crude extracts containing DLPs produced in tetracycline-induced cells but not with those containing DLPs from non-induced cells (Fig. 4b). As treatment with EDTA removed nearly all VP7 molecules, as verified by Western blotting (Fig. 3a), it is unlikely that the observed viroplasms were the consequence of traces of infective TLPs. Indeed, a negative result was obtained by exposing cells to DLPs in the absence of the transfection reagent, ruling out this possibility (data not shown).

From a parallel transfection of DLPs containing VP6–BAP, crude cellular extracts were prepared at 24 h post-transfection and tested for the presence of infective particles. Residual particles still attached to the magnetic beads were removed before infection. Following activation with trypsin, infection of MA104 cells was assessed by detection of viroplasms with anti-NSP5 antibodies. Fig. 4(c) shows that infective viral particles were indeed produced following transfection of the affinity-purified DLPs but not of control beads incubated with material deriving from non-induced cells.

To address whether TLPs containing VP6–BAP were also functional, we determined the infectivity of CsCl-purified TLPs from tetracycline-induced and non-induced cells. The amount of TLPs resulting from each condition used was normalized against VP1 and VP2 content. As shown in Fig. 4(d), TLPs containing biotinylated VP6 were as infective as TLPs not containing the recombinant protein.

In conclusion, whilst an effective and flexible methodology to obtain recombinant rotavirus is not yet available, we have succeeded in incorporating a recombinant viral protein into virions by its overexpression in infected mammalian cells. We have already reported previously the incorporation of a recombinant tagged VP1 protein following a combined transfection and infection procedure (Arnoldi *et al.*, 2007). In this case, viral particles were decorated with biotin on their surface through an *in vivo* biotinylation strategy that can readily be transferred to other viral proteins and to other viruses. In this regard, the *in vivo* biotinylation of the rotavirus spike protein VP4 is under investigation with the aim of obtaining infective biotinylated viral particles. In addition, the viroplasm-resident protein NSP5 has already been shown to be biotinylated successfully *in vivo* (Predonzani *et al.*, 2008), and attempts to use streptavidin-coated magnetic beads to purify viroplasms are ongoing, as these virus factories are still not well characterized.

Several different applications of this technique can be envisaged. For instance, virus tropism may be modified by exploiting the multivalent binding sites of streptavidin to contextually attach biotin-decorated viral particles and

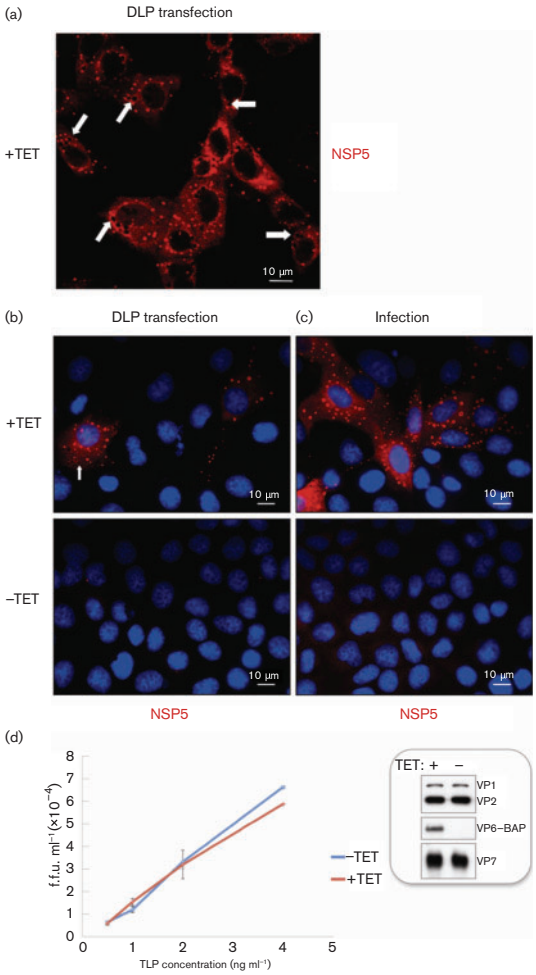

Fig. 4. Viral particles containing VP6–BAP are functional. (a, b) Immunofluorescence with anti-NSP5 antibodies (red) of MA104 cells lipofected with biotinylated DLPs and analysed at 5 h post-transfection. DLPs from tetracycline-induced (a, b; +TET) or non-induced (b; –TET) SA11-infected HEK293/VP6–BAP cells were purified with streptavidin-coated magnetic beads. DLPs were lipofected without being detached from the beads, which are easily recognizable in the fluorescence microscopy images, as indicated by the white arrows. (c) Immunofluorescence with anti-NSP5 antibodies (red) of MA104 cells at 5 h p.i. with viral crude preparations obtained from DLP-lipofected MA104 cells. Viral particles were collected at 24 h post-transfection. (d) Infectivity of normalized equivalent aliquots of CsCl-purified TLPs derived from tetracycline-induced (red line) or non-induced (blue line) HEK293/VP6–BAP cells. The insert shows Western blot analysis of the protein content (VP1, VP2 and VP7) in normalized aliquots of TLPs used for infection experiments.

biotinylated ligands of specific cell-surface internalizing receptors. Moreover, decorated viral particles could be used to sort virus-specific B cells carrying membrane immunoglobulins reacting with virus-assembled proteins within the particle or to identify viral receptors or host-interacting partners.

METHODS

Cells and viruses. MA104 cells and HEK293 cells were grown as monolayers in Dulbecco's modified Eagle's medium (DMEM; Life Technologies) containing 10 % FBS (Life Technologies) and 50 μg gentamicin (Società Prodotti Antibiotici Biodivision) ml^{-1}. Flp-In HEK293 cells (Flp-In T-REx system; Life Technologies), containing the single genomic FRT site for Flp-mediated recombination and transfected for stable expression of the tetracycline repressor (Glatter *et al.*, 2009), were grown in DMEM containing 10 % FBS, 50 μg gentamicin ml^{-1}, 15 μg blasticidin (InvivoGen) ml^{-1} and 100 μg zeocin (InvivoGen) ml^{-1}. Once stably transfected with the pcDNA5-FRT-TO-VP6-BAP-cytBirA plasmid (see below), they were grown in DMEM containing 10 % FBS, 50 μg gentamicin ml^{-1}, 15 μg blasticidin ml^{-1} and 100 μg hygromycin (InvivoGen) ml^{-1}. The simian rotavirus SA11 strain (G3, P6[1]) was propagated in MA104 cells, as described previously (Estes, 2001). Virus titres were determined by immunofluorescence of MA104-infected cells with anti-NSP5 antibodies and expressed as fluorescence-forming units (f.f.u.) ml^{-1}, as described previously (Campagna *et al.*, 2005).

For infectivity assays, normalization of the amount of TLPs from tetracycline-induced and non-induced cells was performed by determination of protein content using a Qubit Protein Assay kit (Life Technologies) and by quantification of VP1 and VP2 content by Western blotting and analysis of the band intensities using ImageJ software (http://rsb.info.nih.gov/ij/).

Quantification of infected cells was performed using an ImageXpress Micro automated high-content screening microscope (Molecular Devices) equipped with a ×20 objective. Automated image analysis of viroplasm formation was performed using MetaXpress software (Molecular Devices) using the Transfluor application module, which identifies cell nuclei and cells containing viroplasms, thus allowing calculation of viral titres.

Construction of plasmids. The VP6-coding sequence was derived from rotavirus SA11 strain (G3, P6[1]) and amplified in two sections by PCR. The first section was obtained using primers VP6(1)for (5′-ACCCAAGCTTGGTACC**A**^{24}TGGATGTCCTA-3′) and VP6(1)rev (5′-ATAGATATCACTTGTCCGGA**C**^{950}GGGAATAGTACTGC-3′ (restriction sites are underlined and superscript numbers indicate the position in the SA11 segment 6 of the nucleotides in bold). The amplicon was cut using restriction enzymes *Hin*dIII and *Eco*RV and inserted into plasmid pcDNA3 (Life Technologies), previously digested with the same enzymes, producing plasmid pcDNA3-VP6/I. The second section was obtained using primers VP6(2)for (5′-ATATCCGGAACTTGGCTAG-C**C**$^{(960)}$CATTCGAACATCATGCA-3′) and VP6(2)rev (5′-ATGGATA-TCT$^{(1217)}$CATTTAATGAGCATGCTTCT-3′) (underlining and superscript numbers as above). The amplicon was cut with *Bsp*EI and *Eco*RV and inserted into plasmid pcDNA3-VP6/I previously digested with the same enzymes, producing plasmid pcDNA3-VP6. The oligonucleotide encoding the BAP peptide (shown in upper case: 5′-ttcggaGG-CCTGAACGATATTTTCGAAGCTCAGAAAATCGAATGGCACGA-Aggcgctagc-3′; restriction sites underlined) was cloned into pcDNA3-VP6 using *Bsp*EI and *Nhe*I, producing plasmid pcDNA3-VP6-BAP. The complete VP6–BAP sequence was transferred into plasmid pcDNA5-FRT-TO (Life Technologies) using *Hin*dIII and *Eco*RV, thus obtaining plasmid pcDNA5-FRT-TO-VP6-BAP.

For cloning of the entire transcriptional unit of the *birA* gene, the bacterial genome was extracted from *E. coli* XL1Blue strain (Stratagene) as follows. The cell pellet was resuspended in TE buffer [50 mM Tris/HCl (pH 8), 20 mM EDTA], the cells were lysed with 2 % Sarcosyl and the protein components were removed by treatment with 500 μg Pronase (Roche) ml^{-1} at 37 °C for 10 min. DNA was extracted with phenol : chloroform : isoamyl alcohol (25 : 24 : 1) and precipitated with 2-propanol. The *birA*-encoding sequence was

amplified using primers BirA-F (5′-CGGAATTCTACCATGAAGG-ATAACACCGTGCCA-3′) and BirA-R (5′-AGACTCGAGTTATTTT-TCTGCACTACGCAGGGA-3′) (restriction sites underlined) and the amplicon was cloned into pcDNA3 using *Eco*RI and *Xho*I, producing plasmid pcDNA3-cytBirA. This was subsequently mutated to create a *Bgl*II site downstream of the transcriptional unit of the *birA* gene in addition to that already present upstream. To obtain plasmid pcDNA5-FRT-TO-VP6-BAP-cytBirA, the entire transcriptional unit of the *birA* gene was first cloned into pcDNA3-VP6-BAP digested with *Bgl*II and then transferred from this plasmid to the pcDNA5-FRT-TO-VP6-BAP vector using *Spe*I digestion.

Molecular images. The image of the VP6 secondary structure of the bovine RF strain of rotavirus (Protein Data Bank accession code 1QHD) was rendered using Visual Molecular Dynamics (VMD) software (Humphrey *et al.*, 1996).

Transfections. The pcDNA5-FRT-TO-VP6-BAP-cytBirA plasmid was transfected transiently in HEK293 cells or stably in Flp-In HEK293 cells by a calcium phosphate technique, as described previously (Eichwald *et al.*, 2004). The stable cell line HEK293/VP6–BAP was obtained by co-transfecting the pOG44 vector encoding Flp (Life Technologies) with pcDNA5-FRT-TO-VP6-BAP-cytBirA. For DLP transfection, DLPs bound to the streptavidin-coated magnetic beads used for their purification (one-twelfth of the purified material was used) were diluted in 100 µl Opti-MEM medium (Life Technologies) and incubated with 4 µg Plus Reagent (Life Technologies) for 5 min at room temperature. Lipofectamine Plus (12 µg; Life Technologies) was then added and, after incubation for 30 min at room temperature, the final mixture was applied to confluent monolayers of MA104 cells in 24-well plates (Ciarlet *et al.*, 2002).

Western blot analysis and retardation assay. Components of cellular extracts and purified viral particles were separated by SDS-PAGE (Laemmli, 1970) using Precision Plus Protein Standards molecular mass markers (Bio-Rad). After electrophoresis, samples were transferred to PVDF membranes (Millipore) (Towbin *et al.*, 1979). The membranes were incubated with the following antibodies (obtained as described previously by Arnoldi *et al.*, 2007 and Contin *et al.*, 2010): anti-VP1 guinea pig serum (diluted 1 : 5000), anti-VP2 guinea pig serum (1 : 5000), anti-VP7 rabbit serum (1 : 1000) and anti-NSP5 guinea pig serum (1 : 8000). The anti-VP6 guinea pig serum (1 : 2500) was kindly provided by Dr Alfred Metzler (Institute of Virology, University of Zurich, Switzerland). For detection of biotinylated VP6–BAP, streptavidin–HRP (1 : 1000; Jackson ImmunoResearch) was used. Membrane stripping was performed using ReBlot Plus Strong Solution (Millipore) following the manufacturer's instructions. To estimate the relative amount of biotinylated versus non-biotinylated VP6–BAP protein, a gel retardation assay was performed, as described previously (Predonzani *et al.*, 2008; Viens *et al.*, 2004). For quantification of the intensity of the bands, ImageJ software was used.

Tetracycline induction and *in vivo* biotinylation. Expression of VP6–BAP was induced in HEK293/VP6–BAP cells by treatment with 1 µg tetracycline (Sigma) ml^{-1} for 24 h before rotavirus infection. Tetracycline induction was performed in the presence of 100 µM biotin (Sigma), which was added to the culture medium to support the *in vivo* biotinylation mediated by the constitutively expressed BirA enzyme (Predonzani *et al.*, 2008).

Purification of viral particles. Viral particles were purified from cell culture when a complete cytopathic effect was reached. The virus was pelleted by ultracentrifugation and the pellet extracted with trichlorotrifluoroethane (Freon; Sigma Aldrich) and separated by ultracentrifugation in a CsCl gradient, as described previously (Patton *et al.*, 2000). Fractions of 500 µl were pelleted and resuspended in 60 µl PIPES buffer (pH 6.6) containing 10 mM $CaCl_2$.

Biotinylated viral particles were purified from fractions of the gradient or directly from crude virus preparations using Dynabeads MyOne Streptavidin T1 (Life Technologies). The magnetic beads were pre-incubated with 1 % BSA in PIPES buffer for 30 min and incubated with the viral particles for 1 h at 4 °C. The beads were washed three times with 0.1 % BSA in PIPES buffer and resuspended in 60 µl PIPES buffer. One-sixth of the purified material was eluted by heating at 95 °C for 15 min and analysed by Western blotting, whereas one-twelfth was used for DLP transfection without detaching the viral particles from the beads.

For purification from crude virus preparations, the virus was pelleted, extracted with Freon, treated with 20 U DNase I (Fermentas) and 20 U RNase ONE (Promega) and finally treated with EDTA as described below. Biotinylated viral particles were isolated using streptavidin-coated magnetic beads, as described above.

EDTA treatment. Virus preparations were dialysed against water and treated with 5 mM EDTA in PIPES buffer for 30 min at 37 °C using a modification of a previously described procedure (Estes *et al.*, 1979). The resulting particles were pelleted by ultracentrifugation and analysed by Western blotting.

Analysis of viral particles by native agarose gel electrophoresis and electroblotting. The viral particle content of TLPs and DLPs was analysed by electrophoresis on a non-denaturing 1 % agarose gel in MOPS buffer (pH 7.25) using a modification of a previously described procedure (Charpilienne *et al.*, 2001). The RNA content of viral particles was revealed by soaking gels in a solution containing 0.1 µg ethidium bromide ml^{-1}. The gels were then incubated for 1 h in transfer buffer [250 mM glycine, 25 mM Tris/HCl (pH 8), 20 % methanol] supplemented with 1 % SDS. Viral proteins were electroblotted onto PVDF membranes (50 mA, overnight). The membranes were then treated as described above for Western blotting.

Fluorescence microscopy. At 5 h p.i. and post-transfection, microscopy experiments were performed as described previously (Eichwald *et al.*, 2002) with the following antibodies: anti-NSP5 guinea pig serum (diluted 1 : 1000) (González & Burrone, 1991), rhodamine (TRITC)-conjugated anti-guinea pig secondary antibody (1 : 200) and streptavidin–Alexa Fluor 488 (1 : 1000) (both from Jackson ImmunoResearch). Cell nuclei were stained with 2 µg Hoechst 33342 (Life Technologies) ml^{-1}. Samples were analysed by confocal microscopy (LSM 510; Carl Zeiss) or using a cool SNAPs system using a fluorescence microscope (DMLB; Leica).

Electron microscopy. DLPs were adsorbed for 10 min to carbon-coated Parlodion films mounted on 300 mesh per inch copper grids (EMS). Samples were washed once with distilled water and stained with saturated uranylacetate (Fluka) for 5 min at room temperature. Specimens were analysed in a transmission electron microscope (CM 12; Philips) equipped with a CCD camera (Ultrascan 1000; Gatan) at an acceleration voltage of 100 kV.

ACKNOWLEDGEMENTS

F. A. was supported by a FIRB grant funded by the Ministero dell'Istruzione, dell'Università e della Ricerca (MIUR), Italy. C. E. and E. M. S. are supported by Canton Zurich to the University of Zürich. We are grateful to Alessandro Vindigni for the kind gift of the Flp-In HEK293 cell line stably expressing the tetracycline repressor, and to Dr Alfred Metzler for the anti-VP6 serum.

REFERENCES

Arnoldi, F., Campagna, M., Eichwald, C., Desselberger, U. & Burrone, O. R. (2007). Interaction of rotavirus polymerase VP1 with nonstructural protein NSP5 is stronger than that with NSP2. *J Virol* **81**, 2128–2137.

Beckett, D., Kovaleva, E. & Schatz, P. J. (1999). A minimal peptide substrate in biotin holoenzyme synthetase-catalyzed biotinylation. *Protein Sci* **8**, 921–929.

Bican, P., Cohen, J., Charpilienne, A. & Scherrer, R. (1982). Purification and characterization of bovine rotavirus cores. *J Virol* **43**, 1113–1117.

Campagna, M., Eichwald, C., Vascotto, F. & Burrone, O. R. (2005). RNA interference of rotavirus segment 11 mRNA reveals the essential role of NSP5 in the virus replicative cycle. *J Gen Virol* **86**, 1481–1487.

Charpilienne, A., Nejmeddine, M., Berois, M., Parez, N., Neumann, E., Hewat, E., Trugnan, G. & Cohen, J. (2001). Individual rotavirus-like particles containing 120 molecules of fluorescent protein are visible in living cells. *J Biol Chem* **276**, 29361–29367.

Charpilienne, A., Lepault, J., Rey, F. & Cohen, J. (2002). Identification of rotavirus VP6 residues located at the interface with VP2 that are essential for capsid assembly and transcriptase activity. *J Virol* **76**, 7822–7831.

Chen, D., Luongo, C. L., Nibert, M. L. & Patton, J. T. (1999). Rotavirus open cores catalyze 5′-capping and methylation of exogenous RNA: evidence that VP3 is a methyltransferase. *Virology* **265**, 120–130.

Chen, J. Z., Settembre, E. C., Aoki, S. T., Zhang, X., Bellamy, A. R., Dormitzer, P. R., Harrison, S. C. & Grigorieff, N. (2009). Molecular interactions in rotavirus assembly and uncoating seen by high-resolution cryo-EM. *Proc Natl Acad Sci U S A* **106**, 10644–10648.

Ciarlet, M., Crawford, S. E., Cheng, E., Blutt, S. E., Rice, D. A., Bergelson, J. M. & Estes, M. K. (2002). VLA-2 ($\alpha 2\beta 1$) integrin promotes rotavirus entry into cells but is not necessary for rotavirus attachment. *J Virol* **76**, 1109–1123.

Contin, R., Arnoldi, F., Campagna, M. & Burrone, O. R. (2010). Rotavirus NSP5 orchestrates recruitment of viroplasmic proteins. *J Gen Virol* **91**, 1782–1793.

Delmas, O., Durand-Schneider, A. M., Cohen, J., Colard, O. & Trugnan, G. (2004). Spike protein VP4 assembly with maturing rotavirus requires a postendoplasmic reticulum event in polarized Caco-2 cells. *J Virol* **78**, 10987–10994.

Dennehy, P. H. (2008). Rotavirus vaccines: an overview. *Clin Microbiol Rev* **21**, 198–208.

Eichwald, C., Vascotto, F., Fabbretti, E. & Burrone, O. R. (2002). Rotavirus NSP5: mapping phosphorylation sites and kinase activation and viroplasm localization domains. *J Virol* **76**, 3461–3470.

Eichwald, C., Rodriguez, J. F. & Burrone, O. R. (2004). Characterization of rotavirus NSP2/NSP5 interactions and the dynamics of viroplasm formation. *J Gen Virol* **85**, 625–634.

Estes, M. (2001). Rotaviruses and their replication. In *Fields Virology*, 4th edn, pp. 1747–1785. Edited by D. Knipe & P. Howley. New York: Lippincott Williams and Wilkins.

Estes, M. K. & Kapikian, A. (2007). Rotaviruses. In *Fields Virology*, 5th edn, pp. 1917–1974. Edited by P. M. Howley, D. M. Knipe, D. A. Griffin, R. A. Lamb, M. A. Martin, B. Roizman & S. E. Straus. Philadelphia: Wolters Kluwer Health/Lippincott Williams & Wilkins.

Estes, M. K., Graham, D. Y., Smith, E. M. & Gerba, C. P. (1979). Rotavirus stability and inactivation. *J Gen Virol* **43**, 403–409.

Feng, N., Lawton, J. A., Gilbert, J., Kuklin, N., Vo, P., Prasad, B. V. & Greenberg, H. B. (2002). Inhibition of rotavirus replication by a non-neutralizing, rotavirus VP6-specific IgA mAb. *J Clin Invest* **109**, 1203–1213.

Glatter, T., Wepf, A., Aebersold, R. & Gstaiger, M. (2009). An integrated workflow for charting the human interaction proteome: insights into the PP2A system. *Mol Syst Biol* **5**, 237.

González, S. A. & Burrone, O. R. (1991). Rotavirus NS26 is modified by addition of single *O*-linked residues of *N*-acetylglucosamine. *Virology* **182**, 8–16.

Humphrey, W., Dalke, A. & Schulten, K. (1996). VMD: visual molecular dynamics. *J Mol Graph* **14**, 33–38, 27–28.

Laemmli, U. K. (1970). Cleavage of structural proteins during the assembly of the head of bacteriophage T4. *Nature* **227**, 680–685.

Lawton, J. A., Estes, M. K. & Prasad, B. V. (1997a). Three-dimensional visualization of mRNA release from actively transcribing rotavirus particles. *Nat Struct Biol* **4**, 118–121.

Lawton, J. A., Zeng, C. Q., Mukherjee, S. K., Cohen, J., Estes, M. K. & Prasad, B. V. (1997b). Three-dimensional structural analysis of recombinant rotavirus-like particles with intact and amino-terminal-deleted VP2: implications for the architecture of the VP2 capsid layer. *J Virol* **71**, 7353–7360.

Lawton, J. A., Estes, M. K. & Prasad, B. V. (1999). Comparative structural analysis of transcriptionally competent and incompetent rotavirus–antibody complexes. *Proc Natl Acad Sci U S A* **96**, 5428–5433.

Lepault, J., Petitpas, I., Erk, I., Navaza, J., Bigot, D., Dona, M., Vachette, P., Cohen, J. & Rey, F. A. (2001). Structural polymorphism of the major capsid protein of rotavirus. *EMBO J* **20**, 1498–1507.

Libersou, S., Siebert, X., Ouldali, M., Estrozi, L. F., Navaza, J., Charpilienne, A., Garnier, P., Poncet, D. & Lepault, J. (2008). Geometric mismatches within the concentric layers of rotavirus particles: a potential regulatory switch of viral particle transcription activity. *J Virol* **82**, 2844–2852.

Liu, M., Mattion, N. M. & Estes, M. K. (1992). Rotavirus VP3 expressed in insect cells possesses guanylyltransferase activity. *Virology* **188**, 77–84.

Mathieu, M., Petitpas, I., Navaza, J., Lepault, J., Kohli, E., Pothier, P., Prasad, B. V., Cohen, J. & Rey, F. A. (2001). Atomic structure of the major capsid protein of rotavirus: implications for the architecture of the virion. *EMBO J* **20**, 1485–1497.

Meyer, J. C., Bergmann, C. C. & Bellamy, A. R. (1989). Interaction of rotavirus cores with the nonstructural glycoprotein NS28. *Virology* **171**, 98–107.

O'Gorman, S., Fox, D. T. & Wahl, G. M. (1991). Recombinase-mediated gene activation and site-specific integration in mammalian cells. *Science* **251**, 1351–1355.

Patton, J., Chizhikov, V., Taraporewala, Z. & Chen, D. Y. (2000). Virus replication. In: *Rotaviruses. Methods and Protocols*, pp. 33–66. Edited by J. Gray & U. Desselberger. Totowa, NJ: Humana Press.

Petris, G., Vecchi, L., Bestagno, M. & Burrone, O. R. (2011). Efficient detection of proteins retro-translocated from the ER to the cytosol by *in vivo* biotinylation. *PLoS ONE* **6**, e23712.

Pizarro, J. L., Sandino, A. M., Pizarro, J. M., Fernández, J. & Spencer, E. (1991). Characterization of rotavirus guanylyltransferase activity associated with polypeptide VP3. *J Gen Virol* **72**, 325–332.

Prasad, B. V., Rothnagel, R., Zeng, C. Q.-Z., Jakana, J., Lawton, J. A., Chiu, W. & Estes, M. K. (1996). Visualization of ordered genomic RNA and localization of transcriptional complexes in rotavirus. *Nature* **382**, 471–473.

Predonzani, A., Arnoldi, F., López-Requena, A. & Burrone, O. R. (2008). *In vivo* site-specific biotinylation of proteins within the secretory pathway using a single vector system. *BMC Biotechnol* **8**, 41.

Settembre, E. C., Chen, J. Z., Dormitzer, P. R., Grigorieff, N. & Harrison, S. C. (2011). Atomic model of an infectious rotavirus particle. *EMBO J* **30**, 408–416.

Taylor, J. A., Meyer, J. C., Legge, M. A., O'Brien, J. A., Street, J. E., Lord, V. J., Bergmann, C. C. & Bellamy, A. R. (1992). Transient expression and mutational analysis of the rotavirus intracellular receptor: the C-terminal methionine residue is essential for ligand binding. *J Virol* **66**, 3566–3572.

Taylor, J. A., O'Brien, J. A., Lord, V. J., Meyer, J. C. & Bellamy, A. R. (1993). The RER-localized rotavirus intracellular receptor: a truncated purified soluble form is multivalent and binds virus particles. *Virology* **194**, 807–814.

Thouvenin, E., Schoehn, G., Rey, F., Petitpas, I., Mathieu, M., Vaney, M. C., Cohen, J., Kohli, E., Pothier, P. & Hewat, E. (2001). Antibody inhibition of the transcriptase activity of the rotavirus DLP: a structural view. *J Mol Biol* **307**, 161–172.

Towbin, H., Staehelin, T. & Gordon, J. (1979). Electrophoretic transfer of proteins from polyacrylamide gels to nitrocellulose sheets: procedure and some applications. *Proc Natl Acad Sci U S A* **76**, 4350–4354.

Valenzuela, S., Pizarro, J., Sandino, A. M., Vásquez, M., Fernández, J., Hernández, O., Patton, J. & Spencer, E. (1991). Photoaffinity labeling of rotavirus VP1 with 8-azido-ATP: identification of the viral RNA polymerase. *J Virol* **65**, 3964–3967.

Viens, A., Mechold, U., Lehrmann, H., Harel-Bellan, A. & Ogryzko, V. (2004). Use of protein biotinylation *in vivo* for chromatin immunoprecipitation. *Anal Biochem* **325**, 68–76.